Title Page

Strand-biased circularizing integrative elements spread *tmexCD-toprJ* gene clusters encoding RND-type multidrug efflux pumps by repeated transpositions

Trung Duc Dao[1&], Hirokazu Yano[2&], Taichiro Takemura[1], Aki Hirabayashi[2], Le Thi Trang[3], Hoang Huy Tran[3], Keigo Shibayama[4], Futoshi Hasebe[1], Ikuro Kasuga[5,6#], and Masato Suzuki[2#]

[1]Vietnam Research Station, Center for Infectious Disease Research in Asia and Africa, Institute of Tropical Medicine, Nagasaki University, Nagasaki, Japan

[2]Antimicrobial Resistance Research Center, National Institute of Infectious Diseases, Tokyo, Japan

[3]National Institute of Hygiene and Epidemiology, Hanoi, Vietnam

[4]Nagoya University Graduate School of Medicine, Nagoya, Japan

[5]Vietnam-Japan University, Vietnam National University, Hanoi, Vietnam

[6]Research Center for Advanced Science and Technology, The University of Tokyo, Tokyo, Japan

[&]Contributed equally

[#]Corresponding authors. E-mail addresses: kasuga@env.t.u-tokyo.ac.jp (I. Kasuga); suzuki-m@niid.go.jp (M. Suzuki)

Keywords: strand-biased circularizing integrative element, SE, *tmexCD-toprJ*, tigecycline, *Aeromonas*

25

26 Running title: SE-mediated transposition mechanism of *tmexCD-toprJ*

27

Abstract

Antimicrobial resistance genes (ARGs) are associated with mobile genetic elements (MGEs) that conscript useful genes into the human–microbe and microbe–microbe battlefields. Thus, under intense selective pressure, ARGs have been constantly adapting and evolving, spreading among microbes. *tmexCD-toprJ* gene clusters, which encode resistance–nodulation–cell division (RND)-type efflux pumps, confer multidrug-resistance to clinically important antimicrobials, including tigecycline. Noteworthily, these gene clusters have emerged in gram-negative bacteria in humans, animals, and the environment worldwide by MGE-mediated transfer. Here we show a hidden MGE, strand-biased circularizing integrative element (SE), that is recently recognized to mediate transpositions of ARGs, associated with the spread of *tmexCD-toprJ* gene clusters. We identified multidrug-resistant isolates of *Aeromonas* species in a water environment in Vietnam that harbored multiple copies of *tmexCD-toprJ* in their chromosomes that were associated with SEs. In particular, *Aeromonas hydrophila* NUITM-VA1 was found to harbor two copies of a novel variant of *tmexC3.3D3.3-topJ1* within cognate SEs, whereas *Aeromonas caviae* NUITM-VA2 harbored four copies of a novel variant of *tmexC2D2.3-topJ2* within cognate SEs. Based on the nature of SE to incorporate a neighboring sequence into the circular form and reinsert it into target sites during transposition, we identified the order of intragenomic movements of *tmexCD-toprJ* gene clusters. Altogether, our findings suggest that most known subgroups of *tmexCD-toprJ* and their subvariants underwent transpositions among bacterial chromosomes and plasmids via SEs. Hence, a *tmexCD-toprJ* gene cluster ancestor may have been

52 initially mobilized via SE, subsequently spreading among bacteria and evolving

53 in new hosts.

54

Introduction

Antimicrobial resistance genes (ARGs) are estimated to have originated in environmental bacteria and subsequently spread to pathogenic bacteria in humans as acquired ARGs (1). Mobile genetic elements (MGEs) are the major driving force of gene transfer and amplification underlying ARG evolution (2). Spontaneous mutations and antimicrobial selection have led to the emergence of clinically problematic ARGs, including carbapenemase genes (*e.g.* bla_{NDM}, bla_{KPC}, $bla_{OXA\text{-}48\text{-}like}$, bla_{IMP}, bla_{VIM}, and $bla_{GES\text{-}5\text{-}like}$) (3), colistin resistance genes (*e.g. mcr* and *arnT*) (4, 5), and tigecycline resistance genes [*e.g. tet*(X) and *tmexCD-toprJ*] (6).

Carbapenem, colistin, and tigecycline are considered last-resort antimicrobials for infections caused by multidrug-resistant (MDR) gram-negative bacteria, such as *Enterobacterales*, *Pseudomonas aeruginosa*, and *Acinetobacter baumannii*, which are serious global public health threats (3, 4, 6). *tet*(X4) and other *tet*(X) variants, which encode flavin-dependent monooxygenases that catalyze tigecycline degradation, have emerged mainly in *Enterobacterales* and *Acinetobacter* species (3). *tmexCD1-toprJ1*, *tmexCD2-toprJ2*, *tmexCD3-toprJ1* (initially designated *tmexCD3-toprJ3*), *tmexCD4-toprJ4*, and other *tmexCD-toprJ* subvariants, which encode resistance–nodulation–cell division (RND)-type efflux pumps that excrete multiple antimicrobials, including tigecycline, have emerged worldwide mainly in *Enterobacterales* and *Pseudomonas* species (3, 7–16).

Recently, a novel MGE family, named strand-biased circularizing integrative element (SE), was identified in *Vibrio alfacsensis* (17) and later in more diverse taxa of *Gammaproteobacteria* (18). SEs move between genomic locations via a

79 copy-out-like route using tyrosine recombinases: SEs incorporate 6 bases next
80 to the 5′-end of one specific strand into their circular intermediate form, which are
81 then reinserted into a new target location. Therefore, SE-mediated transposition
82 results in the insertion of 6 bases at newly formed *attR* recombination sites (17),
83 and this 6-bp footprints allow tracing the order of SE integration events that
84 occurred in the past in a genome.

85 In this study, we investigated MDR bacteria in a water environment in Vietnam
86 and found MDR isolates of *Aeromonas* species that harbored multiple genes
87 conferring resistance to last-resort antimicrobials, including *tmexCD-toprJ* gene
88 clusters. Close examination of MGEs associated with multiple copies of *tmexCD-*
89 *toprJ* in the chromosomes indicated involvement of SEs in the intragenomic
90 amplification of the gene clusters. Comparison of sequences around known
91 variants of *tmexCD-toprJ* in publicly available genome data revealed that most of
92 them were likely integrated into bacterial chromosomes and plasmids via SEs.
93

Results and Discussion

Two carbapenem- and tigecycline-resistant isolates of *Aeromonas* species, namely NUITM-VA1 and NUITM-VA2, respectively, were obtained from a water environment in Vietnam in 2021. Whole-genome sequencing analysis revealed that NUITM-VA1 (accession no. AP025277) and NUITM-VA2 (accession no. AP025280) were 97.1% and 97.9% identical to *Aeromonas hydrophila* strain ATCC 7966^T (accession no. CP000462) and *Aeromonas caviae* strain CECT 838^T (accession no. JAGDEN000000000), respectively. Multilocus sequence typing analysis revealed that NUITM-VA1 and NUITM-VA2 belonged to novel sequence types (STs), ST1063 and ST1064, respectively, of *Aeromonas* species.

A. hydrophila NUITM-VA1 harbored multiple clinically important ARGs, such as intrinsic genes of cephalosporinase (bla_{cepH}) and oxacillinase (bla_{aphH}), tigecycline resistance genes [*tet*(X4) and *tmexCD3-toprJ1*-like], phosphoethanolamine transferase gene conferring colistin resistance (*mcr-3.9*), and efflux pump gene conferring fluoroquinolone resistance (*qnrVC4*), whereas *A. caviae* NUITM-VA2 harbored carbapenemase genes (bla_{NDM-1}, bla_{KPC-2}, and bla_{VIM-4}), tigecycline resistance genes (*tmexCD2-toprJ2*-like), and 16S ribosomal RNA methyltransferase gene conferring aminoglycoside resistance (*rmtB*) (Figs. 1A and B). Noteworthily, NUITM-VA1 and NUITM-VA2 harbored multiple copies of tigecycline resistance genes. Consistent with this observation, NUITM-VA1 and NUITM-VA2 showed low susceptibility to most antimicrobials tested, including carbapenems, cephalosporins, aminoglycosides, fluoroquinolone, and colistin with some exceptions (Table 1).

Indeed, two copies of *tmexCD3-toprJ1*-like gene clusters and four copies of *tet*(X4) (including the pseudogene) associated with the insertion sequence IS*CR2* were identified in NUITM-VA1, whereas four copies of *tmexCD2-toprJ2*-like gene clusters were identified in NUITM-VA2 (Fig. 1A and B). The identity for *tmexC3*, *tmexD3*, and *toprJ1* in NUITM-VA1 with the corresponding component genes of *tmexCD3-toprJ1* (accession no. CP066833) (10) were 99.91% (with one amino acid substitution, T235A), 99.90% (with V56E, Q283H, and G591V substitutions), and 100%, respectively. The identity for *tmexC2*, *tmexD2*, and *toprJ2* in NUITM-VA2 with the corresponding component genes of *tmexCD2-toprJ2* (accession no. CP054471) (9) were 100%, 99.97% (with V56E substitution), and 100%, respectively.

Recently, several subvariants of genes comprised in the *tmexCD-toprJ* cluster were identified, including *tmexD1.2* (*tmexD1* variant with V64I substitution) in *Klebsiella pneumoniae* pC5921_mex (IncFIB/IncHI1B/IncU plasmid, accession no. MZ532979) and *tmexD2.2* (*tmexD2* variant with V56E and P382A substitutions) in *Klebsiella oxytoca* pC7532_mex (IncFII/IncU plasmid, accession no. MZ532981) (15). In addition, known gene variants of the representative *tmexCD-toprJ* cluster (Table 2), including *tmexC3.2* (*tmexC3* variant with Q187H, T256M, and A386T substitutions) and *tmexD3.2* (*tmexD3* variant with V610L and L611F substitutions) in *Klebsiella aerogenes* pNUITM-VK5_mdr (IncC/IncX3 plasmid, accession no. LC633285) identified in our previous study (11). Based on these naming-standards, we designated the novel variants of *tmexCD-toprJ* identified in NUITM-VA1 and NUITM-VA2 as *tmexC3.3D3.3-toprJ1* and *tmexC2D2.3-toprJ2*, respectively.

To elucidate the molecular mechanism of intragenomic transposition of *tmexCD-toprJ*, comparative analysis among *tmexCD-toprJ*-containing genomic regions in NUITM-VA1 and NUITM-VA2 was performed. Overall, *tmexCD-toprJ* and the regulator gene *tnfxB* encoded upstream of the gene cluster were found to be associated with an atypical MGE family, SE, that consists of four conserved genes of integrases (*intA* and *intB*), tyrosine recombinase-fold protein (*tfp*), and SE-associated recombination auxiliary protein (*srap*) (17, 18) (Figs. 1C and D).

In NUITM-VA1, one copy of *tmexC3.3D3.3-toprJ1*-containing SE was flanked by 5′-CATCGA-3′ in *attL* and 5′-TATCGA-3′ in *attR*, whereas the other SE copy was flanked by 5′-TATCGA-3′ and 5′-CATCGA-3′ (Figs. 1A and C). Given the nature of the 6-bp footprint of SE transposition (17, 18), it is likely that one SE copy became the donor for the other SE copy in the second location in NUITM-VA1, but the donor location could not be defined. In NUITM-VA2, four copies of *tmexC2D2.3-toprJ2*-containing SEs were detected in the chromosome. The 6-bp fingerprint 5′-TATCGA-3′ was identified next to the 5′-end of the SE copy at the location #1 (4,079,313–4,062,461 nt), as well as next to the 3′-end of the SE copy at the location #2 (3,001,983–3,018,834 nt), and the other SE copy at the location #3 (2,130,980–2,114,127 nt) (Figs. 1B and D). Thus, the SE copy at the location #1 was likely the donor of the other SE copies at locations #2 and #3. Moreover, the 6-bp fingerprint 5′-TATCGA-3′ was identified next to the 5′-end of the SE copy at location #2, as well as next to the 3′-end of the SE copy at the location #4 (1,131,379–1,114,526 nt), suggesting that the SE copy at the location #2 was the donor of the SE copy at the location #4.

Importantly, identical structures as those of *tmexC3.3D3.3-toprJ1*-containing SE in NUITM-VA1 and *tmexC2D2.3-toprJ2*-containing SE in NUITM-VA2 were detected in chromosomes of *A. caviae* WCW1-2 (accession no. CP039832) (19) and *A. caviae* K333 (accession no. CP084031) (20), respectively. Moreover, the *tet*(X4)-containing region in NUITM-VA1 was also detected in the WCW1-2 chromosome, suggesting that these genetic structures around ARGs in *Aeromonas* species isolates herein described are not an unusual event.

The known *tmexCD-toprJ* gene cluster can be divided into four major subgroups, consisting of *tmexCD1-toprJ1*, *tmexCD2-toprJ2*, *tmexCD3-toprJ1*, and *tmexCD4-toprJ4* (3, 7–16). Hence, the presence of SEs in these *tmexCD-toprJ* subgroups and their subvariants was examined next (Fig. 2). The intact sequences of *tnfxB-tmexCD-toprJ*-containing SEs were identified in all subgroups except *tmexCD4-toprJ4* (Fig. 2A). Although some SEs, such as *tmexCD2-toprJ2*-containing SEs in *Raoultella ornithinolytica* NC189 (accession no. CP054471 and MN175502) (9), *tmexC2D2.3-toprJ2*-containing SE in *A. caviae* NUITM-VA2 in this study, and *tmexC3D3-toprJ1*-containing SE in *Pseudomonas terrae* subsp. *cibarius* SDQ8C180-2T (accession no. CP073356) (12), harbored insertions of other MGEs within their SEs, such as insertion sequences, the 5'- and 3'-end of the SEs were completely conserved, indicating that they can form functional mobility structures. Interestingly, IncP-2 megaplasmids, such as *P. aeruginosa* pBT2436 (accession no. CP039989) (14, 21), was previously suggested to frequently carry *tmexCD-toprJ*; thus, plasmids also seemed to be involved in such SE-mediated transpositions.

Broken structures close to *tmexCD-toprJ*-containing SEs that lacked the conserved genes of SE and *tmexCD-toprJ*-associated *tnfxB* were also detected (Fig. 2B). This type of broken structures may have concealed the herein described close relationship between *tmexCD-toprJ* and SEs in previous studies. For example, *tmexCD1-toprJ1* in *K. pneumoniae* pMH15-269M_1 (IncFIB/HI1B plasmid, accession no. AP023338) (8) and *Citrobacter portucalensis* pHN21SC92-1 (IncC plasmid, accession no. CP089438) (16) was previously suspected of being mobilized by IS*26*, but intact 3'-end sequence of SE was present on pMH15-269M_1 but not on pHN21SC92-1, suggesting the involvement of other MGEs rather than SE is an event that occurred after initial SE-mediated transpositions. For *tmexCD4-toprJ4* in *Klebsiella quasipneumoniae* pHNLW22-2 (untypeable plasmid, accession no. CP089443) (13), no evidence suggested SE involvement on either the 3' or 5' sides of the gene cluster; nevertheless, since this *tmexCD-toprJ* variant has only been reported in one case to date, a possible association with SE cannot be ruled out.

In conclusion, our present study provides a glimpse into *Aeromonas* species, one of the most common environmental bacteria that have been rapidly and silently becoming resistant to clinically important antimicrobials. Notably, our present study highlights for the first time the role of SE-mediated transpositions for the evolution of the MDR gene clusters, *tmexCD-toprJ*. Our previous study suggested that *Aeromonas* and *Pseudomonas* species in the natural environment are not only important reservoirs of ARGs, but are also carriers of evolutionary changes in ARGs, such as $bla_{\text{GES-5}}$-like carbapenemase genes (22). The MGE-mediated spread of ARGs among bacteria and their epidemiology

211 concerning some specific examples, such as *mcr1* and IS*Apl1* (23), and *bla*$_{NDM}$
212 and Tn*125* (24), have been previously analyzed in detail. The present study
213 provides more direct epidemiological evidence of transpositions of *tmexCD-toprJ*
214 mediated by SEs, which can be identified by the footprints of SEs. This finding is
215 quite significant for investigating the global spreading of ARGs, including
216 *tmexCD-toprJ*, and will pave the way for future genomic epidemiological
217 investigations on antimicrobial-resistant bacteria.
218

Materials and methods

Bacterial isolation and antimicrobial susceptibility testing

Carbapenem- and tigecycline-resistant of environmental isolates of *Aeromonas* species, *A. hydrophila* NUITM-VA1 and *A. caviae* NUITM-VA2 were obtained from the Kim-Nguu River in Hanoi, Vietnam, in March 2021. Environmental water sample was collected and cultured using Luria-Bertani (LB) broth containing 4 mg/L of meropenem at 37°C overnight, and then further selected and isolated using CHROMagar COL-APSE (CHROMagar Microbiology) containing 4 mg/L of tigecycline. Bacterial species identification was performed using MALDI Biotyper (Bruker). Antimicrobial susceptibility testing using *Escherichia coli* ATCC 25922 as quality control was performed with agar dilution according to the CLSI 2020 guidelines. For tigecycline, AST was additionally performed in the presence or absence of 75 mg/L of the efflux pump inhibitor 1-(1-naphthylmethyl)-piperazine (NMP) as used in the previous studies (7, 11) .

Whole-genome sequencing and subsequent bioinformatics analysis

Whole-genome sequencing of NUITM-VA1 and NUITM-VA2 was performed using MiSeq (Illumina) with MiSeq Reagent Kit v2 (300-cycle) and MinION (Oxford Nanopore Technologies; ONT) with the R9.4.1 flow cell. The library for Illumina sequencing (paired-end, insert size of 300–800 bp) was prepared using the Nextera XT DNA Library Prep Kit, and the library for MinION sequencing was prepared using the Rapid Barcoding Kit (SQK-RBK004). ONT reads were basecalled using Guppy v5.0.11 in the super-accuracy mode and then

243 assembled de novo using Canu v2.1.1 (https://github.com/marbl/canu) with the
244 default parameters. The overlap regions in the assembled contigs were detected
245 using LAST (https://gitlab.com/mcfrith/last) and then trimmed manually.
246 Sequencing errors were corrected by Racon v1.4.20
247 (https://github.com/isovic/racon) twice with the default parameters using ONT
248 reads and then corrected by Pilon v1.20.1
249 (https://github.com/broadinstitute/pilon) twice with the default parameters using
250 Illumina reads, resulting in their complete circular chromosomes.
251 Genome annotation and average nucleotide identity analyses were performed
252 using the DFAST server (https://dfast.nig.ac.jp). ARGs were detected using
253 Staramr v0.7.2 (https://github.com/phac-nml/staramr) with the custom ARGs
254 database, including all known tigecycline resistance genes. The circular
255 representation of bacterial chromosomes was visualized using the Proksee
256 server (https://proksee.ca). Linear comparison of sequence alignments of
257 genomic regions containing ARGs and MGEs was performed using BLAST and
258 visualized by Easyfig v2.2.2 (http://mjsull.github.io/Easyfig/).
259

Nucleotide sequence accession nos.

Complete chromosome sequences of *A. hydrophila* NUITM-VA1 and *A. caviae* NUITM-VA2 have been deposited at GenBank/EMBL/DDBJ under accession nos. AP025277 and AP025280, respectively.

Funding

This work was supported by grants (JP22gm1610003, JP22fk0108133, JP22fk0108139, JP22fk0108642, JP22wm0225004, JP22wm0225008, JP22wm0225022, JP22wm0325003, JP22wm0325022, and JP22wm0325037 to M. Suzuki; JP22fk0108132 and JP22wm0225008 to I. Kasuga; JP22wm0125006 and JP22wm0225008 to F. Hasebe; JP22fk0108604 and JP22gm1610003 to K. Shibayama) from the Japan Agency for Medical Research and Development (AMED), grants (20K07509 and 21K18742 to M. Suzuki; 19K21984 and 21K18742 to I. Kasuga; 21K18742 to T. Takemura; 21K15440 to A. Hirabayashi) from the Ministry of Education, Culture, Sports, Science and Technology (MEXT), Japan, a grant from Mishima Kaium Memorial Foundation to H. Yano, and a grant (MS.108.02-2017.320 to H. H. Tran) from the National Foundation for Science and Technology Development (NAFOSTED), Vietnam.

Competing interests

None declared.

Ethical approval

Not required.

References

1. Davies J, Davies D. 2010. Origins and evolution of antibiotic resistance. Microbiol Mol Biol Rev 74:417-33.
2. Sandegren L, Andersson DI. 2009. Bacterial gene amplification: implications for the evolution of antibiotic resistance. Nat Rev Microbiol 7:578-88.
3. Diene SM, Rolain JM. 2014. Carbapenemase genes and genetic platforms in Gram-negative bacilli: Enterobacteriaceae, Pseudomonas and Acinetobacter species. Clin Microbiol Infect 20:831-8.
4. Mmatli M, Mbelle NM, Osei Sekyere J. 2022. Global epidemiology, genetic environment, risk factors and therapeutic prospects of mcr genes: A current and emerging update. Front Cell Infect Microbiol 12:941358.
5. Gallardo A, Iglesias MR, Ugarte-Ruiz M, Hernandez M, Miguela-Villoldo P, Gutierrez G, Rodriguez-Lazaro D, Dominguez L, Quesada A. 2021. Plasmid-mediated Kluyvera-like arnBCADTEF operon confers colistin (hetero)resistance to Escherichia coli. Antimicrob Agents Chemother.
6. Anyanwu MU, Nwobi OC, Okpala COR, Ezeonu IM. 2022. Mobile Tigecycline Resistance: An Emerging Health Catastrophe Requiring Urgent One Health Global Intervention. Front Microbiol 13:808744.
7. Lv L, Wan M, Wang C, Gao X, Yang Q, Partridge SR, Wang Y, Zong Z, Doi Y, Shen J, Jia P, Song Q, Zhang Q, Yang J, Huang X, Wang M, Liu JH. 2020. Emergence of a Plasmid-Encoded Resistance-Nodulation-

306 Division Efflux Pump Conferring Resistance to Multiple Drugs, Including
307 Tigecycline, in Klebsiella pneumoniae. mBio 11.
308 8. Hirabayashi A, Ha VTT, Nguyen AV, Nguyen ST, Shibayama K, Suzuki M.
309 2021. Emergence of a plasmid-borne tigecycline resistance in Klebsiella
310 pneumoniae in Vietnam. J Med Microbiol 70.
311 9. Wang CZ, Gao X, Yang QW, Lv LC, Wan M, Yang J, Cai ZP, Liu JH. 2021.
312 A Novel Transferable Resistance-Nodulation-Division Pump Gene Cluster,
313 tmexCD2-toprJ2, Confers Tigecycline Resistance in Raoultella
314 ornithinolytica. Antimicrob Agents Chemother 65.
315 10. Wang Q, Peng K, Liu Y, Xiao X, Wang Z, Li R. 2021. Characterization of
316 TMexCD3-TOprJ3, an RND-Type Efflux System Conferring Resistance to
317 Tigecycline in Proteus mirabilis, and Its Associated Integrative Conjugative
318 Element. Antimicrob Agents Chemother 65:e0271220.
319 11. Hirabayashi A, Dao TD, Takemura T, Hasebe F, Trang LT, Thanh NH,
320 Tran HH, Shibayama K, Kasuga I, Suzuki M. 2021. A Transferable IncC-
321 IncX3 Hybrid Plasmid Cocarrying blaNDM-4, tet(X), and tmexCD3-toprJ3
322 Confers Resistance to Carbapenem and Tigecycline. mSphere
323 6:e0059221.
324 12. Wang CZ, Gao X, Lv LC, Cai ZP, Yang J, Liu JH. 2021. Novel tigecycline
325 resistance gene cluster tnfxB3-tmexCD3-toprJ1b in Proteus spp. and
326 Pseudomonas aeruginosa, co-existing with tet(X6) on an SXT/R391

integrative and conjugative element. J Antimicrob Chemother 76:3159-3167.

13. Gao X, Wang C, Lv L, He X, Cai Z, He W, Li T, Liu JH. 2022. Emergence of a Novel Plasmid-Mediated Tigecycline Resistance Gene Cluster, tmexCD4-toprJ4, in Klebsiella quasipneumoniae and Enterobacter roggenkampii. Microbiol Spectr 10:e0109422.

14. Shintani M, Suzuki H, Nojiri H, Suzuki M. 2022. Precise classification of antimicrobial resistance-associated IncP-2 megaplasmids for molecular epidemiological studies on Pseudomonas species. J Antimicrob Chemother 77:1203-1205.

15. Sun S, Wang Q, Jin L, Guo Y, Yin Y, Wang R, Bi L, Zhang R, Han Y, Wang H. 2022. Identification of multiple transfer units and novel subtypes of tmexCD-toprJ gene clusters in clinical carbapenem-resistant Enterobacter cloacae and Klebsiella oxytoca. J Antimicrob Chemother 77:625-632.

16. Liu YY, Gao X, He X, Lv L, Jiao Y, Yu R, Liu JH. 2022. Emergence of the tigecycline resistance gene cluster tmexCD1-toprJ1 in an IncC plasmid and Citrobacter portucalensis. J Antimicrob Chemother 77:2030-2033.

17. Nonaka L, Masuda M, Yano H. 2022. Atypical integrative element with strand-biased circularization activity assists interspecies antimicrobial resistance gene transfer from Vibrio alfacsensis. PLoS One 17:e0271627.

18. Idola D, Mori H, Nagata Y, Nonaka L, Yano H. 2022. Host range of strand-biased circularizing integrative elements: a new class of mobile

DNA elements nesting in Gammaproteobacteria. Research Square. DOI: https://doi.org/10.21203/rs.3.rs-1499202/v1

19. Chen C, Chen L, Zhang Y, Cui CY, Wu XT, He Q, Liao XP, Liu YH, Sun J. 2019. Detection of chromosome-mediated tet(X4)-carrying Aeromonas caviae in a sewage sample from a chicken farm. J Antimicrob Chemother 74:3628-3630.

20. Luo X, Mu K, Zhao Y, Zhang J, Qu Y, Hu D, Jia Y, Dai P, Weng J, Wang D, Yu L. 2022. Emergence of bla NDM- 1-Carrying Aeromonas caviae K433 Isolated From Patient With Community-Acquired Pneumonia. Front Microbiol 13:825389.

21. Cazares A, Moore MP, Hall JPJ, Wright LL, Grimes M, Emond-Rheault JG, Pongchaikul P, Santanirand P, Levesque RC, Fothergill JL, Winstanley C. 2020. A megaplasmid family driving dissemination of multidrug resistance in Pseudomonas. Nat Commun 11:1370.

22. Maehana S, Eda R, Hirabayashi A, Niida N, Nakamura M, Furukawa T, Ikeda S, Kojima F, Sakai K, Sei K, Kitasato H, Suzuki M. 2021. Natural factories that manufacture antimicrobial resistance genes: quadruple blaGES-carrying plasmids in Aeromonas and Pseudomonas species. Int J Antimicrob Agents 57:106327.

23. Wang R, van Dorp L, Shaw LP, Bradley P, Wang Q, Wang X, Jin L, Zhang Q, Liu Y, Rieux A, Dorai-Schneiders T, Weinert LA, Iqbal Z, Didelot X,

Wang H, Balloux F. 2018. The global distribution and spread of the mobilized colistin resistance gene mcr-1. Nat Commun 9:1179.

24. Acman M, Wang R, van Dorp L, Shaw LP, Wang Q, Luhmann N, Yin Y, Sun S, Chen H, Wang H, Balloux F. 2022. Role of mobile genetic elements in the global dissemination of the carbapenem resistance gene blaNDM. Nat Commun 13:1131.

25. Jiang X, Yin Z, Yuan M, Cheng Q, Hu L, Xu Y, Yang W, Yang H, Zhao Y, Zhao X, Gao B, Dai E, Song Y, Zhou D. 2020. Plasmids of novel incompatibility group IncpRBL16 from Pseudomonas species. J Antimicrob Chemother 75:2093-2100.

381 **Legends**

382 **Table 1.** MICs of antimicrobials against *A. hydrophila* NUITM-VA1 and *A. caviae*
383 NUITM-VA2. The efflux pump inhibitor 1-(1-naphthylmethyl)-piperazine (NMP)
384 was used at 75 mg/L. Abbreviations: TIG, tigecycline; MIN, minocycline; DOX,
385 doxycycline; TET, tetracycline; IPM, imipenem; MEM, meropenem; CTX,
386 cefotaxime; CAZ, ceftazidime; CIP, ciprofloxacin; AMK, amikacin; GEN,
387 gentamicin; TOB, tobramycin; STR, streptomycin; CST, colistin.

388

389 **Table 2.** All known variants of mobile RND-type efflux pump gene clusters,
390 *tmexCD-toprJ*. Subgroups and subvariants of *tmexCD-toprJ*, types of component
391 proteins (TMexC, TMexD, and TOprJ), bacterial isolate/plasmid harboring the
392 corresponding *tmexCD-toprJ*, accession nos., and references are shown.

393

394 **Fig. 1.** (A and B) Circular representation of chromosomes of *A. hydrophila*
395 NUITM-VA1 (accession no. AP025277) (A) and *A. caviae* NUITM-VA2
396 (accession no. AP025280) (B) isolated in Vietnam in 2021 in this study. The
397 dashed arrows indicate the putative order of SE-mediated transpositions of *tnfxB-*
398 *tmexCD-toprJ*. (C and D) Linear comparison of *tmexCD-toprJ*-containing SEs
399 and *tet*(X4)-containing regions in *A. hydrophila* NUITM-VA1 (C) and *A. caviae*
400 NUITM-VA2 (D) with those of *A. caviae* WCW1-2 (accession no. CP039832)
401 isolated from an environment in China in 2018 (19) and *A.caviae* K333 (accession
402 no. CP084031) isolated from a human in China in 2020 (20). 5'- and 3'-ends of
403 SEs and their 6-bp transposition footprint sequences in *Aeromonas* species
404 isolates in this study are shown. Red, yellow, light green, light blue, gray, green,

purple, and black indicate carbapenem and tigecycline resistance genes (CRG and TRG), other antimicrobial resistance genes (ARG), mobile gene elements (MGE), type IV secretion system-associated genes involved in conjugation (T4SS), other coding sequences (Other), GC Skew+, GC Skew–, and GC content, respectively. The blue color in comparison of sequences indicates almost 100% identity.

Fig. 2. Linear comparison of *tmexCD-toprJ*-containing SEs in *A. hydrophila* NUITM-VA1 and *A. caviae* NUITM-VA2 (accession nos. AP025277 and AP025280, respectively) isolated in Vietnam in 2021 in this study with the intact (A) or broken forms (B) in previously reported sequences of *K. pneumoniae* AHM7C8I plasmid pHNAH8I-1 (accession no. MK347425) isolated from an animal in China in 2017 (7), *R. ornithinolytica* NC189 and the plasmid pHNNC189-2 (accession nos. CP054471 and MN175502, respectively) isolated from a human in China in 2018 (9), *P. mirabilis* RGF134-1 (accession no. CP066833) isolated from an animal in China in 2019 (10), *P. terrae* subsp. *cibarius* SDQ8C180-2T (accession no. CP073356) isolated from an animal in China in 2018 (12), *P. aeruginosa* T2436 plasmid pBT2436 (accession no. CP039989) isolated from a human in Thailand in 2013 (14, 25), *K. pneumoniae* MH15-269M plasmid pMH15-269M_1 (accession no. AP023338) isolated from a human in Vietnam in 2015 (8), *C. portucalensis* GD21SC92T plasmid pHN21SC92-1 (accession no. CP089438) isolated from an environment in China in 2021 (16), *P. aeruginosa* 1705-19119 plasmid p519119-DIM (accession no. MN208061) isolated in China in 2017 (14, 24), *K. aerogenes* NUITM-VK5 plasmid

pNUITM-VK5_mdr (accession no. LC633285) isolated from an environment in Vietnam in 2021 (11), and *K. quasipneumoniae* GLW9C22 plasmid pHNLW22-2 (accession no. CP089443) isolated from an animal in China in 2019 (13). Red, yellow, light blue, and gray indicate *tmexCD-toprJ* gene clusters (*tmexCD-toprJ*), other antimicrobial resistance genes (ARG), mobile gene elements (MGE), and other coding sequences (Other), respectively. The color in comparison of sequences shows the indicated % of identity.

437 **Table 1.**

Isolate	MIC (mg/L)													
	TIG (+NMP)	MIN	DOX	TET	IPM	MEM	CTX	CAZ	CIP	AMK	GEN	TOB	STR	CST
A. hydrophila NUITM-VA1	64 (8)	64	128	>128	0.5	0.5	128	>128	>128	>128	128	>128	128	4
A. caviae NUITM-VA2	8 (1)	128	128	>128	64	32	>128	>128	>128	>128	>128	>128	>128	0.25
E. coli ATCC 29522	0.125 (0.125)	1	2	2	0.25	0.032	0.125	0.5	0.008	2	0.5	1	0.5	0.125

438

439 **Table 2.**

Subgroup	Subvariant	TMexC	TMexD	TOprJ	Bacterial isolate/plasmid	Accession no.	Reference
tmexCD1-toprJ1	*tmexCD1-toprJ1*	TMexC1	TMexD1	TOprJ1	*K. pneumoniae* pHNAH8I-1	MK347425	(7)
	tmexCD1.2-toprJ1	TMexC1	TMexD1.2 (V64I of TMexD1)	TOprJ1	*K. pneumoniae* pC5921_mex	MZ532979	(15)
tmexCD2-toprJ2	*tmexCD2-toprJ2*	TMexC2	TMexD2	TOprJ2	*R. ornithinolytica* NC189	CP054471	(9)
	tmexC2D2.2-toprJ2	TMexC2	TMexD2.2 (V56E and P382A of TMexD2)	TOprJ2	*K. oxytoca* pC7532_mex	MZ532981	(15)
	tmexC2D2.3-toprJ2	TMexC2	TMexD2.3 (V56E of TMexD2)	TOprJ2	*A. caviae* NUITM-VA2	AP025280	This study
	tmexC2.2D2-toprJ2.2	TMexC2.2 (Y15C, I17V, R31G, K45Q, F52V, and E108Q of TMexC2)	TMexD2	TOprJ2.2 (A47T and L1177P of TOprJ2)	*P. aeruginosa* p519119-DIM	MN208061	(14, 24)
tmexCD3-toprJ1	*tmexCD3-toprJ1*	TMexC3	TMexD3	TOprJ1	*P. mirabilis* RGF134-1	CP066833	(10)
	tmexC3.2D3.2-toprJ1	TMexC3.2 (Q187H, T256M, and A386T of TMexC3)	TMexD3.2 (V610L and L611F of TMexD3)	TOprJ1	*K. aerogenes* pNUITM-VK5_mdr	LC633285	(11)
	tmexC3.3D3.3-toprJ1	TMexC3.3 (T235A of TMexC3)	TMexD3.3 (V56E, Q283H, and G591V of TMexD3)	TOprJ1	*A. hydrophila* NUITM-VA1	AP025277	This study
	tmexC3.3D3-toprJ1	TMexC3.3 (T235A of tmexC3)	TMexD3	TOprJ1	*P. aeruginosa* pBT2436	CP039989	(14, 25)
tmexCD4-toprJ4	*tmexCD4-toprJ4*	TMexC4	TMexD4	TOprJ4	*K. quasipneumoniae* pHNLW22-2	CP089443	(13)

440

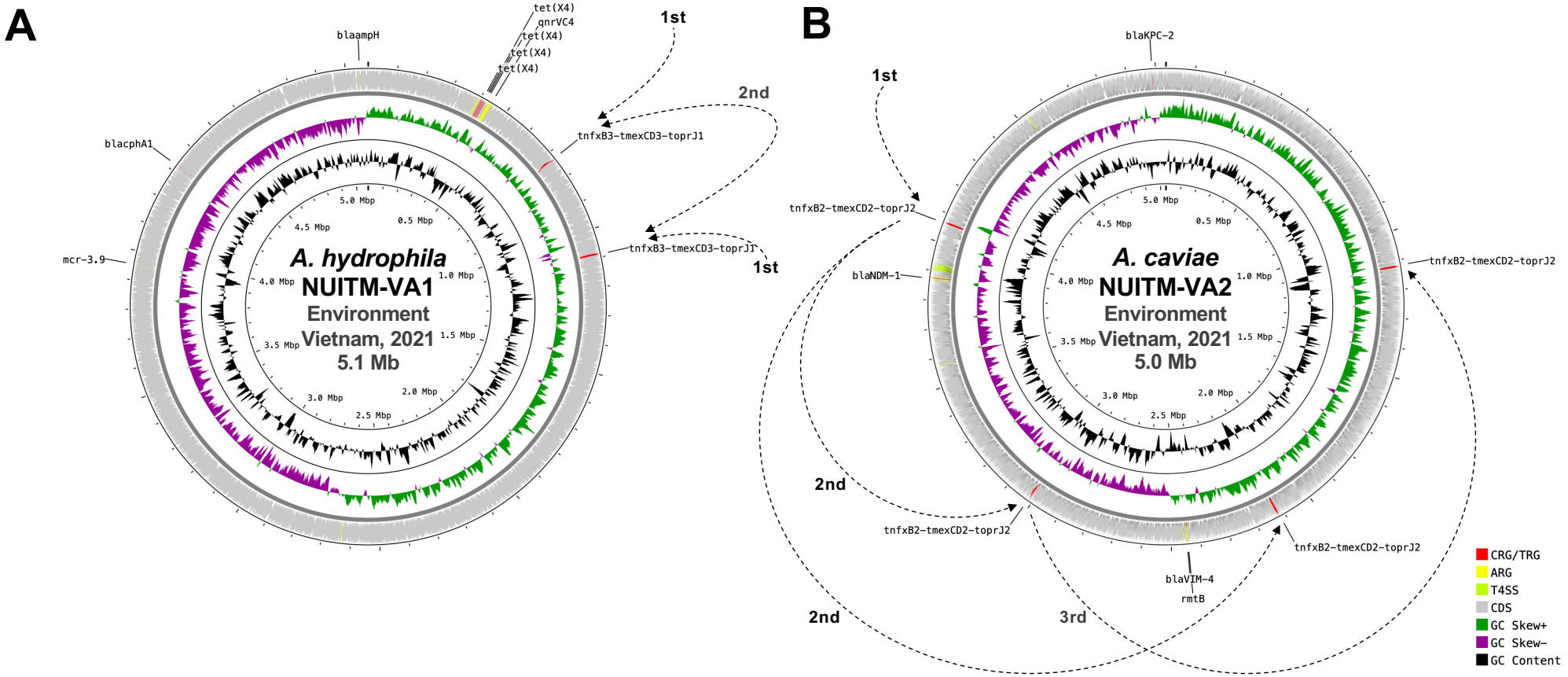
A
blaampH
tet(X4)
qnrVC4
tet(X4)
tet(X4)
tet(X4)
1st
2nd
tnfxB3-tmexCD3-toprJ1
tnfxB3-tmexCD3-toprJ1
1st
blacphA1
mcr-3.9
A. hydrophila
NUITM-VA1
Environment
Vietnam, 2021
5.1 Mb
B
blaKPC-2
1st
tnfxB2-tmexCD2-toprJ2
blaNDM-1
tnfxB2-tmexCD2-toprJ2
A. caviae
NUITM-VA2
Environment
Vietnam, 2021
5.0 Mb
2nd
tnfxB2-tmexCD2-toprJ2
tnfxB2-tmexCD2-toprJ2
blaVIM-4
rmtB
2nd
3rd
CRG/TRG
ARG
T4SS
CDS
GC Skew+
GC Skew−
GC Content
C
SE-tmexC3.3D3.3-toprJ1
A. hydrophila
NUITM-VA1
(Chromosome: 738,209 – 722,581 nt)
A. hydrophila
NUITM-VA1
(Chromosome: 1,077,200 – 1,092,829 nt)
A. caviae
WCW1-2
Environment, China, 2018
(Chromosome: 1,344,686 – 1,329,057 nt)
A. hydrophila
NUITM-VA1
(Chromosome: 404,769 – 426,239 nt)
A. caviae
WCW1-2
Environment, China, 2018
(Chromosome: 2,069,724 – 2,073,620 nt)
5'-end of SE
3'-end of SE
intA
tfp
intB
srap
tnfxB3
tmexC3.3
tmexD3.3
toprJ1
ISVsa3
abh
tet(X4)
ISCR2
ISVSAs20
pseudogenes
D
SE-tmexC2D2.3-toprJ2
A. caviae
NUITM-VA2
(Chromosome: 4,079,313 – 4,062,461 nt)
A. caviae
NUITM-VA2
(Chromosome: 3,001,983 – 3,018,834 nt)
A. caviae
NUITM-VA2
(Chromosome: 2,130,980 – 2,114,127 nt)
A. caviae
NUITM-VA2
(Chromosome: 1,131,379 – 1,114,526 nt)
A. caviae
K333
Human, China, 2020
(Chromosome: 3,796,328 – 3,779,474 nt)
5' end of SE
3' end of SE
intA
tfp
intB
srap
tnfxB2
ISBvi2
tmexC2
tmexD2.3
toprJ2
pseudogenes
TRG
ARG
MGE
Other

Fig. 1

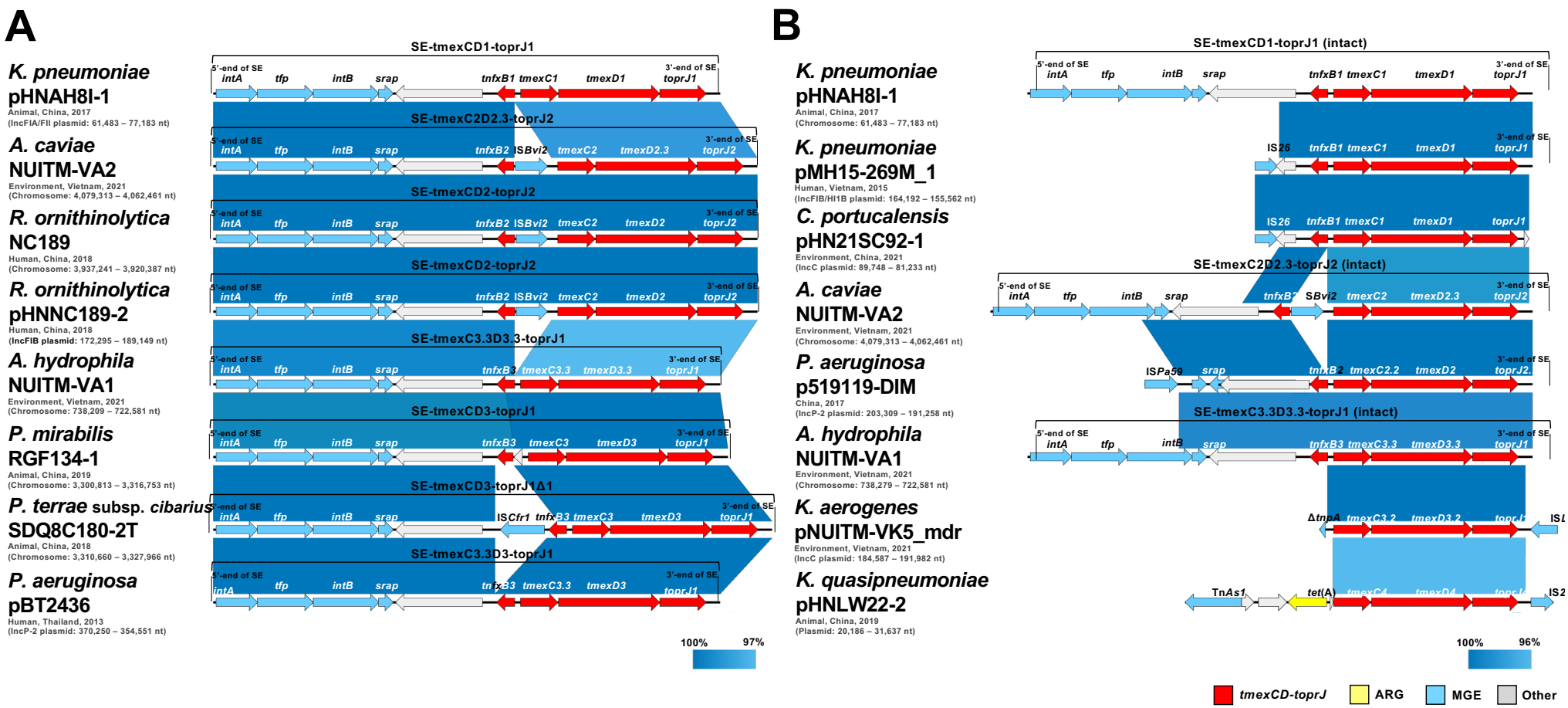
A
K. pneumoniae
pHNAH8I-1
Animal, China, 2017
(IncFIA/FII plasmid: 61,483 – 77,183 nt)
A. caviae
NUITM-VA2
Environment, Vietnam, 2021
(Chromosome: 4,079,313 – 4,062,461 nt)
R. ornithinolytica
NC189
Human, China, 2018
(Chromosome: 3,937,241 – 3,920,387 nt)
R. ornithinolytica
pHNNC189-2
Human, China, 2018
(IncFIB plasmid: 172,295 – 189,149 nt)
A. hydrophila
NUITM-VA1
Environment, Vietnam, 2021
(Chromosome: 738,209 – 722,581 nt)
P. mirabilis
RGF134-1
Animal, China, 2019
(Chromosome: 3,300,813 – 3,316,753 nt)
P. terrae subsp. cibarius
SDQ8C180-2T
Animal, China, 2018
(Chromosome: 3,310,660 – 3,327,966 nt)
P. aeruginosa
pBT2436
Human, Thailand, 2013
(IncP-2 plasmid: 370,250 – 354,551 nt)
SE-tmexCD1-toprJ1
SE-tmexC2D2.3-toprJ2
SE-tmexCD2-toprJ2
SE-tmexCD2-toprJ2
SE-tmexC3.3D3.3-toprJ1
SE-tmexCD3-toprJ1
SE-tmexCD3-toprJ1Δ1
SE-tmexC3.3D3.3-toprJ1
5'-end of SE
3'-end of SE
intA
tfp
intB
srap
tnfxB1
tmexC1
tmexD1
toprJ1
tnfxB2
ISBvi2
tmexC2
tmexD2.3
toprJ2
tmexD2
tnfxB3
tmexC3.3
tmexD3.3
tmexC3
tmexD3
ISCfr1
100%
97%
B
K. pneumoniae
pHNAH8I-1
Animal, China, 2017
(Chromosome: 61,483 – 77,183 nt)
K. pneumoniae
pMH15-269M_1
Human, Vietnam, 2015
(IncFIB/HI1B plasmid: 164,192 – 155,562 nt)
C. portucalensis
pHN21SC92-1
Environment, China, 2021
(IncC plasmid: 89,748 – 81,233 nt)
A. caviae
NUITM-VA2
Environment, Vietnam, 2021
(Chromosome: 4,079,313 – 4,062,461 nt)
P. aeruginosa
p519119-DIM
China, 2017
(IncP-2 plasmid: 203,309 – 191,258 nt)
A. hydrophila
NUITM-VA1
Environment, Vietnam, 2021
(Chromosome: 738,279 – 722,581 nt)
K. aerogenes
pNUITM-VK5_mdr
Environment, Vietnam, 2021
(IncC plasmid: 184,587 – 191,982 nt)
K. quasipneumoniae
pHNLW22-2
Animal, China, 2019
(Plasmid: 20,186 – 31,637 nt)
SE-tmexCD1-toprJ1 (intact)
SE-tmexC2D2.3-toprJ2 (intact)
SE-tmexC3.3D3.3-toprJ1 (intact)
IS26
ISPa59
ΔtnpA
TnAs1
tet(A)
100%
96%
tmexCD-toprJ
ARG
MGE
Other

Fig. 2